Supplementary Materials

Uniform mesoporous Nb_2O_5 microspheres with controlled porosity for efficient lithium storage

Lanhao Yang[1,#], Dafu Tang[2,#], Rongyao Li[1], Jingyu Zhang[1], Wendi Wang[1], Jialong Li[1], Yalin He[1], Xiu Wen[1], Qiulong Wei[2,*], Kun Lan[1,*]

[1]College of Energy Materials and Chemistry, College of Chemistry and Chemical Engineering, Inner Mongolia University, Hohhot 010021, Inner Mongolia, China.
[2]Department of Materials Science and Engineering, College of Materials, Xiamen University, Xiamen 361000, Fujian, China.
[#]Authors contributed equally.

[*]**Correspondence:** Prof. Kun Lan, College of Energy Materials and Chemistry, College of Chemistry and Chemical Engineering, Inner Mongolia University, Hohhot 010021, Inner Mongolia, China. E-mail: k_lan@imu.edu.cn; Prof. Qiulong Wei, Department of Materials Science and Engineering, College of Materials, Xiamen University, Xiamen 361000, Fujian, China. E-mail: qlwei@xmu.edu.cn

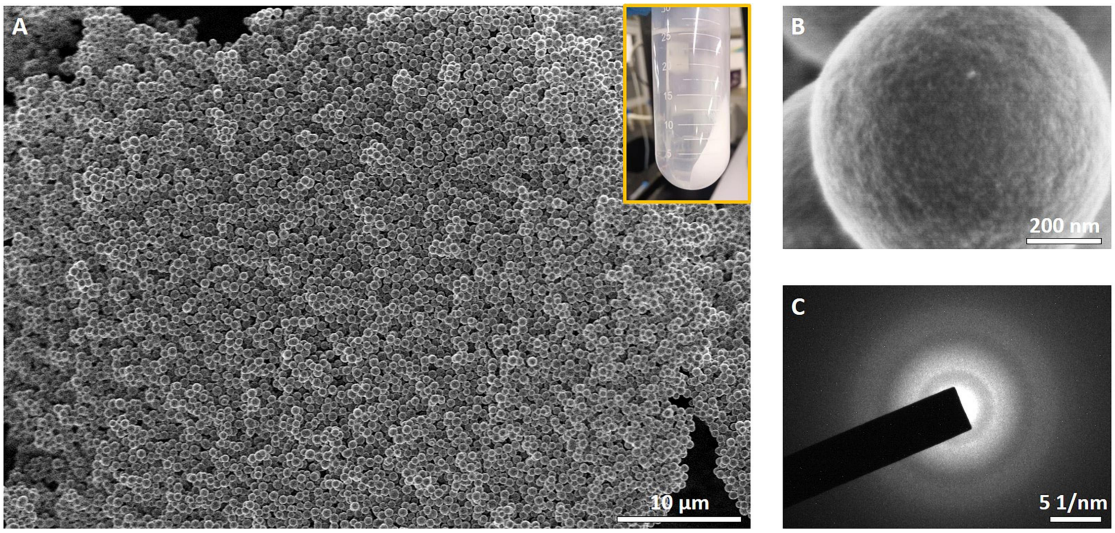

Supplementary Figure 1. Characterization of the as-made mesoporous Nb_2O_5 microspheres: (A) Large-area and (B) High-magnification SEM images of the as-made mesoporous Nb_2O_5 microspheres (Inset: Photographic image after centrifugation); (C) SAED pattern of the as-made mesoporous Nb_2O_5 microspheres.

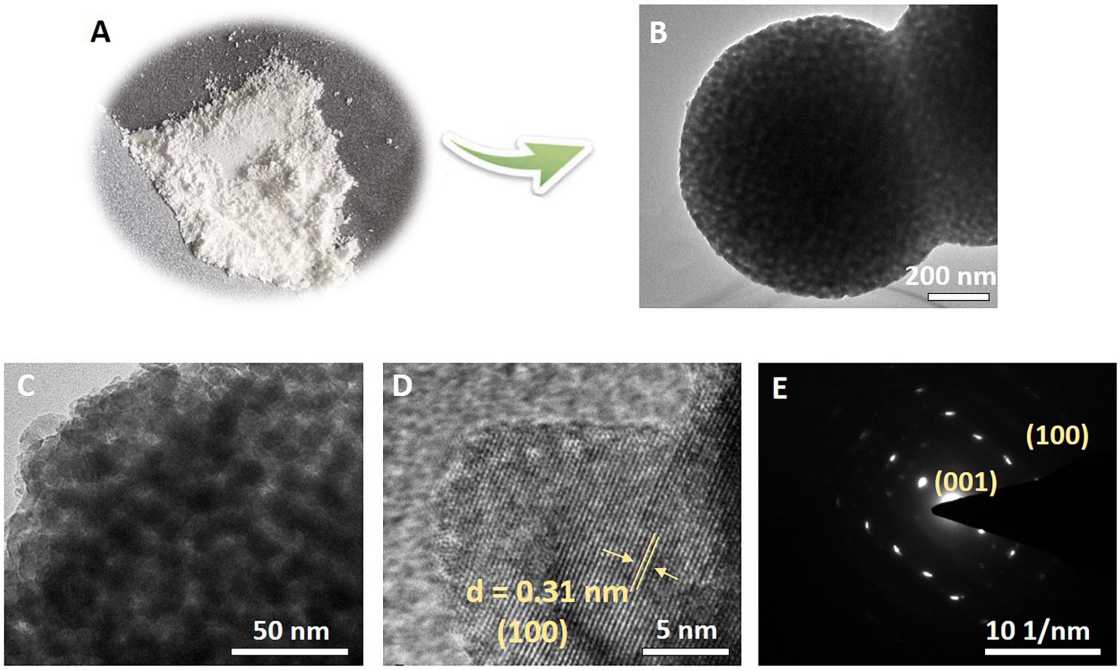

Supplementary Figure 2. Characterization of the mesoporous Nb_2O_5 microspheres after calcination. (A) Photographic image of the mesoporous Nb_2O_5 microspheres; (B and C) TEM images, (D) HRTEM image, and (E) SAED pattern of the mesoporous Nb_2O_5 microspheres.

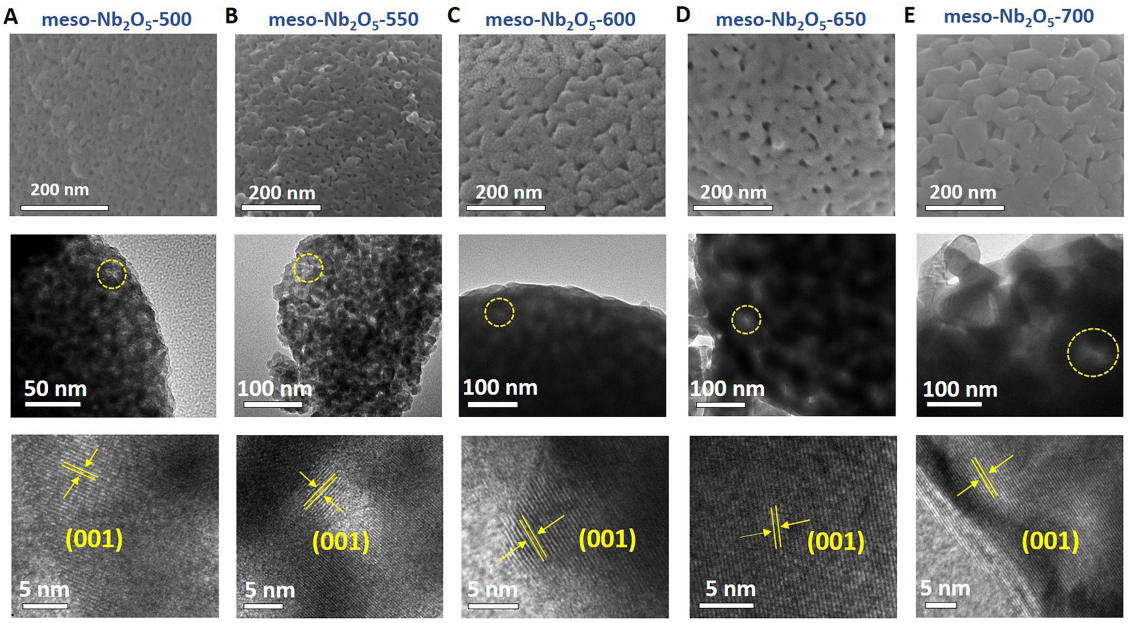

Supplementary Figure 3. (A-E) SEM, TEM and HRTEM images of the mesoporous Nb_2O_5 microspheres calcined in air at different temperatures from 500 to 700 °C.

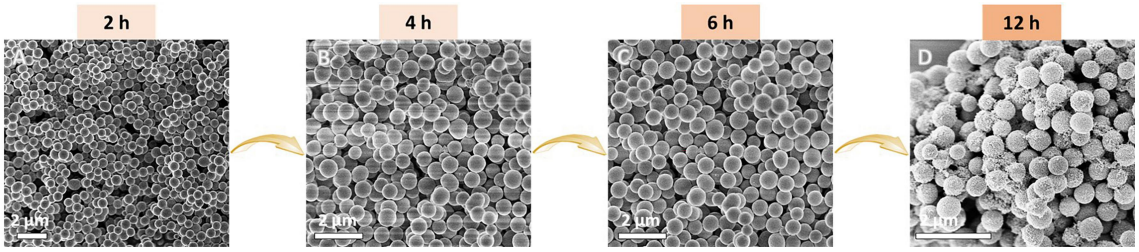

Supplementary Figure 4. Intermediate observation at different hydrothermal time intervals. (A-D) SEM images of the as-made mesoporous Nb_2O_5 microspheres harvested at different hydrothermal time intervals.

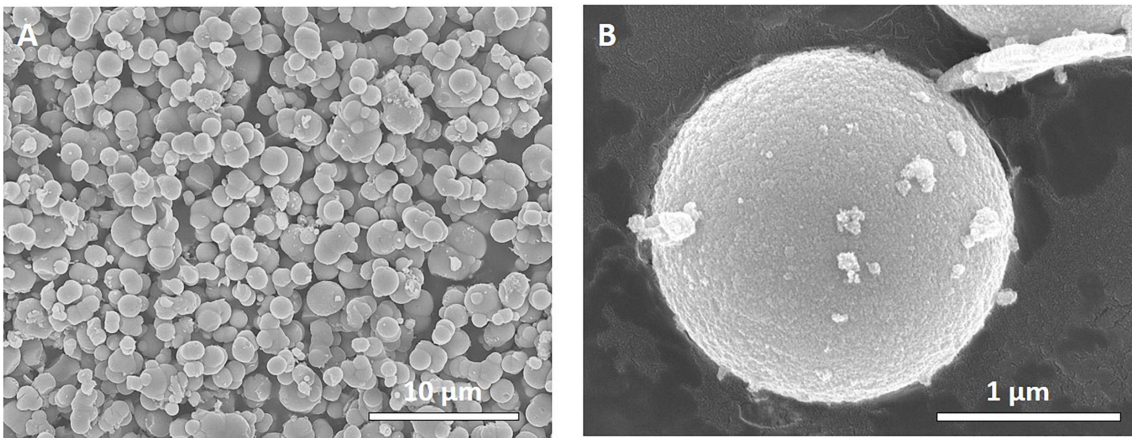

Supplementary Figure 5. (A) Low-magnification and (B) High-magnification SEM images of the mesoporous Nb_2O_5 microspheres obtained using 60 mL of ethanol.

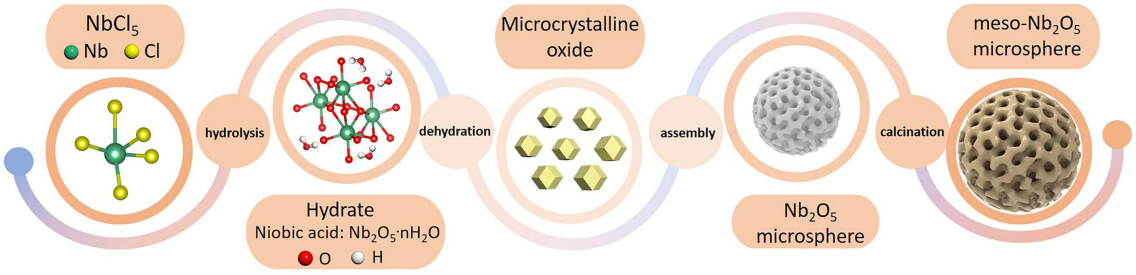

Supplementary Figure 6. Schematic diagram for the formation process of mesoporous Nb_2O_5 microspheres.

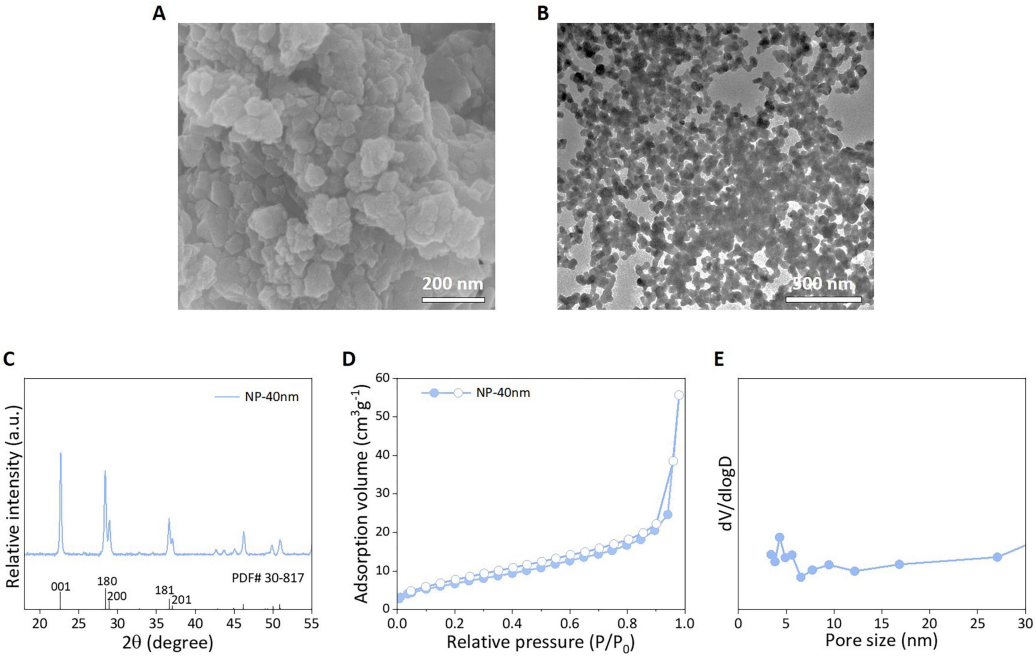

Supplementary Figure 7. (A) SEM and (B) TEM images of the loose Nb_2O_5 nanoparticles; (C) The XRD pattern, (D) Nitrogen adsorption-desorption isotherms, and (E) Pore size distribution curve of the loose Nb_2O_5 nanoparticles.

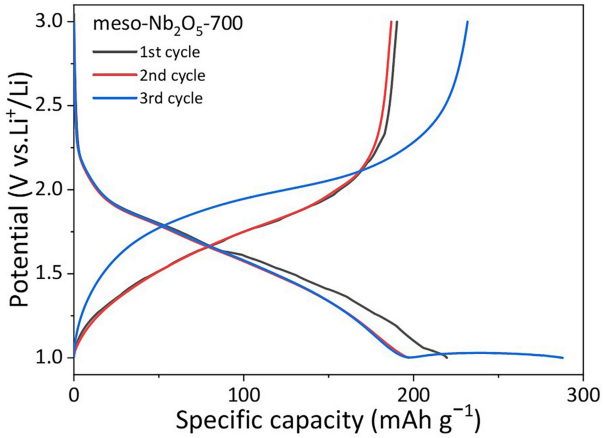

Supplementary Figure 8. Charge and discharge curves of the meso-Nb_2O_5-700 in the potential range of 1-3 V *vs.* Li^+/Li.

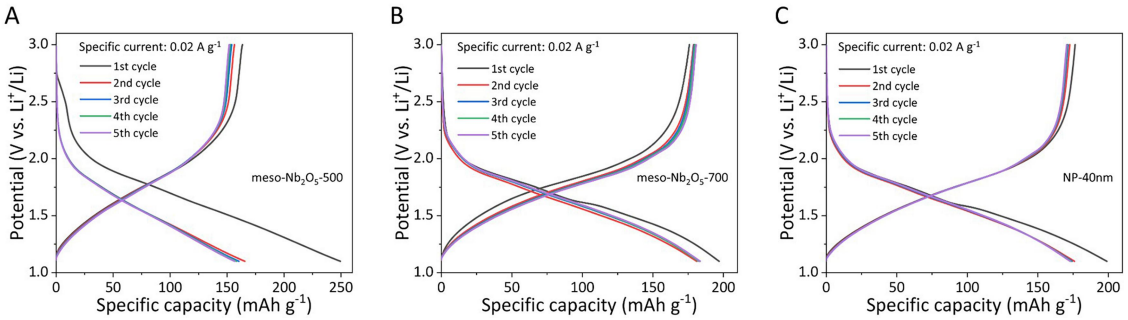

Supplementary Figure 9. Galvanostatic charge-discharge curves of the (A) meso-Nb_2O_5-500, (B) meso-Nb_2O_5-700, and (C) NP-40 nm electrodes in the 2nd cycle at the specific current of 0.02 A g^{-1}.

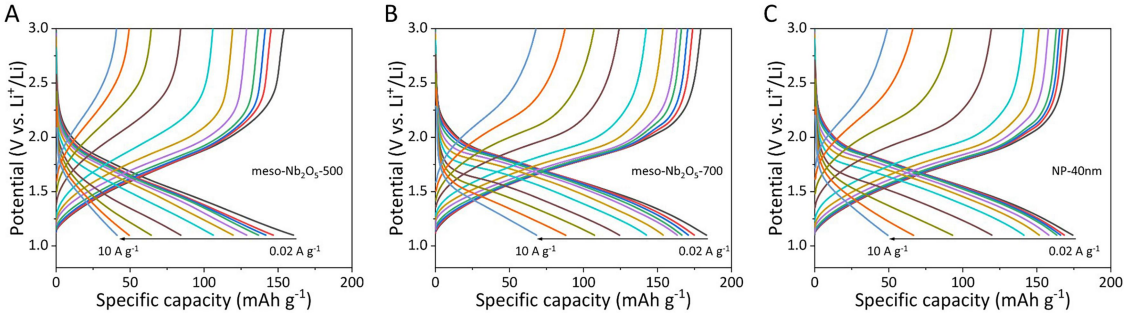

Supplementary Figure 10. Galvanostatic charge-discharge curves of (A) the meso-Nb_2O_5-500, (B) meso-Nb_2O_5-700, and (C) NP-40 nm electrodes at different specific currents ranging from 0.02 to 10 A g^{-1}.

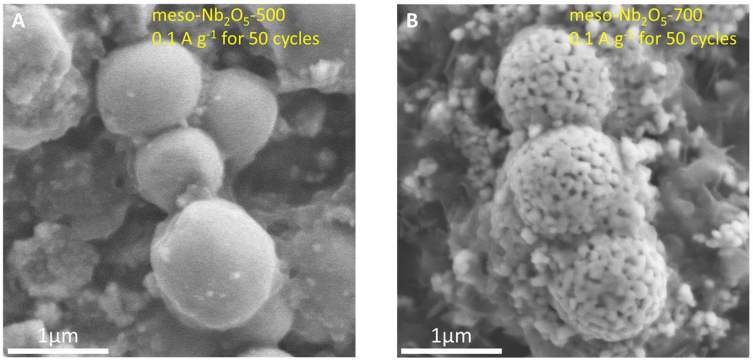

Supplementary Figure 11. SEM images of the (A) meso-Nb_2O_5-500 and (B) meso-Nb_2O_5-700 electrodes after 50 cycles at 0.1 A g^{-1}.

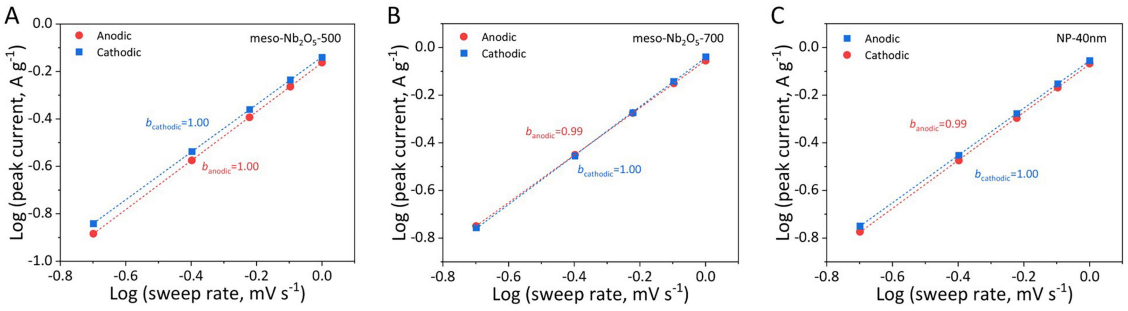

Supplementary Figure 12. *b*-value fittings of anodic and cathodic peaks of (A) the meso-Nb_2O_5-500, (B) meso-Nb_2O_5-700, and (C) NP-40 nm electrodes.

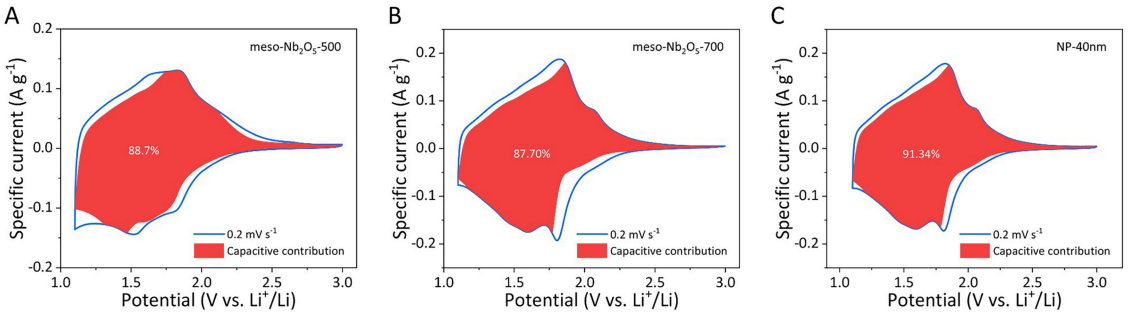

Supplementary Figure 13. The simulated capacity contribution of the (A) meso-Nb_2O_5-500, (B) meso-Nb_2O_5-700, and (C) NP-40 nm electrodes at a scan rate of 0.2 mVs^{-1}.

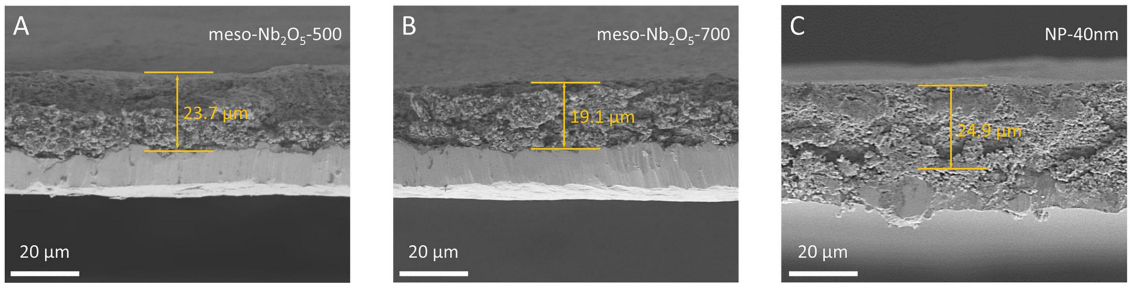

Supplementary Figure 14. Cross-section SEM images of (A) the meso-Nb_2O_5-500, (B) meso-Nb_2O_5-700, and (C) NP-40 nm electrodes.

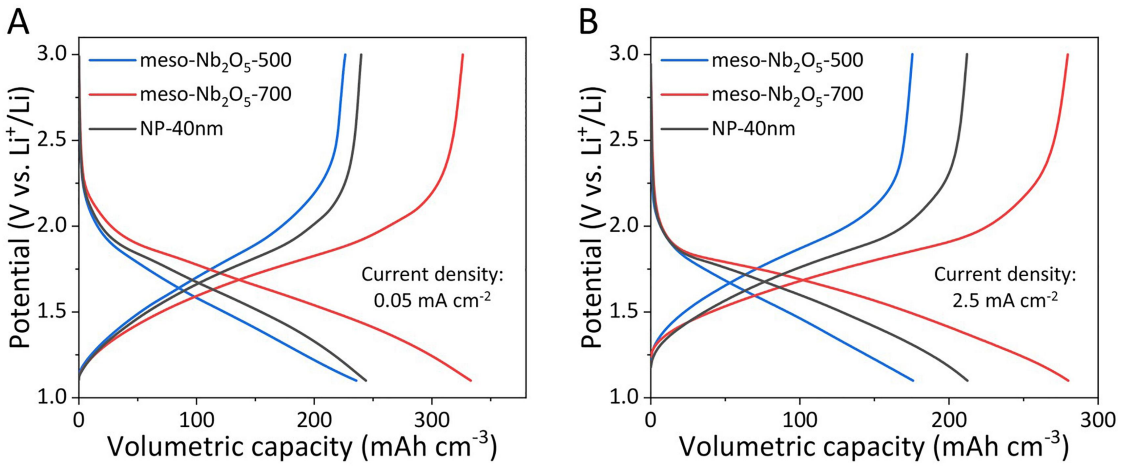

Supplementary Figure 15. Galvanostatic charge-discharge curves of the meso-Nb_2O_5-500, meso-Nb_2O_5-700, and NP-40 nm electrodes at a current density of (A) 0.05 mA cm^{-2} and (B) 2.5 mA cm^{-2}.

Supplementary Table 1. Structural properties of the mesoporous Nb_2O_5 samples after calcination at different temperatures in air

Calcination temperature (°C)	Average grain[a] size (nm)	Mesopore size (nm)	Surface area (m^2/g)	Pore volume (cm^3/g)
500	33.5	7.7	93	0.16
550	44.1	8.1	79	0.18
600	48.8	15.6	41	0.15
650	59.2	25.8	27	0.17
700	61.7	45.0	10	0.11

[a]The average grain sizes of samples were calculated based on Scherrer equation: $D=K\lambda/(\beta\cos\theta)$, where K is constant, λ is the X-ray wavelength, β is the diffraction peak at half height and width, and θ is the diffraction angle. The background of XRD patterns is subtracted; after smoothing correction, the peak width is calculated based on the (001) peak.

Supplementary Table 2. Detailed data for calculating the compaction density

Electrode	Electrode area(cm^2)	Electrode material thickness (μm)	Electrode material mass (mg)	Compaction density[a] (g cm^{-3})
meso-Nb_2O_5-500	1.13	23.7	3.93	1.47
meso-Nb_2O_5-700	1.13	19.1	3.93	1.82
NP-40nm	1.13	24.9	3.93	1.4

[a]The compaction densities of all samples were calculated based on the cross-section SEM image (Supplementary Figure 12) and using: $\rho = m/hS$, where ρ (g cm^{-3}) is the compaction density, m (g) is the total mass of materials, h (cm) is the thickness of materials, and S (cm^2) is the electrode area.